Robust Design Optimization of Surface-Mounted Permanent Magnet Synchronous Motor Using Uncertainty Characterization by Bootstrap Method

Saekyeol Kim, Soo-Gyung Lee, Ji-Min Kim, Tae Hee Lee, *Member, IEEE*, and Myung-Seop Lim, *Member, IEEE*

***Abstract*—The uncertainty of electric machines and drives is inherent in its manufacturing and assembly. Robust design optimization finds the design under these uncertainties that results in a minimal variance while satisfying all design constraints. To obtain an accurate result, the statistical model is significantly important. Moreover, several uncertainties from a single source can be involved owing to multiple components in the electrical machines and drives. However, this can drastically increase the numerical cost for the conventional robust design optimization technique. In this work an uncertainty characterization method is developed by using a percentile bootstrap interval to consider the experimental results from few prototypes and a kriging surrogate model to reduce the computational cost. Then the sample-based robust design optimization is applied to the surface-mounted permanent magnet synchronous motor. It is seen that the developed methods can efficiently work to minimize both the mean and variance of the cogging torque while satisfying other design constraints.**

***Index Terms*—Kriging surrogate model, percentile bootstrap interval, robust design optimization, surface-mounted permanent magnet synchronous motor, uncertainty characterization.**

I. Introduction

UNCERTAINTY in electric machines and drives is unavoidably inherent in the manufacturing process. Because of various uncertainties, these products usually exhibit variance in their characteristics and performances. In the worst-case scenario, this phenomenon can even lead to the production of defective electromagnetic devices. These uncertainties generally come from the manufacturing and assembly tolerance, and material properties. To improve the robustness of electric machines and drives under various uncertainties, a large number of design optimization methods have been developed in recent years [1], [2]. The purpose of robust design optimization (RDO) is to find the least sensitive design under uncertainties that results in a minimal variance while satisfying all design constraints [3].

The electrical power steering (EPS) system has become an attractive alternative to conventional hydraulic power steering in automotive vehicles, owing to its significant contribution to the reduction in weight and fuel consumption. The cogging torque is the torque that is generated owing to the interaction between the permanent magnets of the rotor and stator slots of the electric motor. Minimizing the cogging torque is the most important design objective with regard to the EPS motors because it considerably affects the handling performance of vehicles. The cogging torque usually shows a large variation under uncertainties originating from the manufacturing process [4]–[8].

Although several RDO techniques have been developed and adopted for various electromagnetic devices, they are usually based on the assumption that input uncertainties follow a normal distribution [9]–[12]. Moreover, the standard deviation of these uncertainties is determined based on the designer's experience. As these assumptions cause significant errors in the RDO results, the probability distribution and its statistical parameters should be accurately determined. However, the characterization or identification of these uncertainties is extremely difficult, especially at the initial design stage.

Another important design issue is that electric machines and drives include components that are produced from the same manufacturing process, e.g., permanent magnets or a segmented stator core. After production, these components are assembled into a single product. Therefore, the combined effect of the uncertainties caused by multiple components is different from that of a single component [8]. Many studies disregarded this design aspect because electromagnetic simulations were usually performed using symmetry models in which these uncertainties were treated as a single random variable. This issue is a challenging problem that cannot be resolved using conventional RDO techniques because they deal with each uncertainty based on different design variable or parameter [3], [13].

To resolve these two issues, this study proposes two novel methods: an uncertainty characterization method using finite element analysis (FEA) and experimental data from prototype testing, and an RDO method that considers uncertainties of

Manuscript received January 14, 2020; revised May 6, 2020; accepted June 9, 2020. Date of publication June 23, 2020; date of current version November 24, 2020. *(Corresponding author: Tae Hee Lee.)*

Saekyeol Kim, Soo-Gyung Lee, Tae Hee Lee, and Myung-Seop Lim are with the Department of Automotive Engineering, Hanyang University, Seoul 04763, South Korea (e-mail: kyeol8805@gmail.com; sgar1109@hanyang.ac.kr; thlee@hanyang.ac.kr; myungseop@hanyang.ac.kr).

Ji-Min Kim is with the Department of Automotive Engineering, Hanyang University, Seoul 04763, South Korea, and also with the Digital Appliances, Samsung Electronics, Suwon 16677, South Korea (e-mail: jimin85.kim@samsung.com).

Color versions of one or more of the figures in this article are available online at https://ieeexplore.ieee.org.

Digital Object Identifier 10.1109/TEC.2020.3004342

multiple components. To improve the accuracy of the uncertainty characterization, numerous prototypes are required. This is not a feasible option in most cases owing to the associated high cost. To address the lack of information, the bootstrap method is adopted to calculate the confidence intervals (CIs) of mean and standard deviation using the available few experimental data. Thus, the uncertainty characterization can be performed considering all the possible scenarios based on few prototypes. The optimization that minimizes the difference between the mean values obtained from the bootstrap method and simulation is performed to find the fittest probability distribution and its parameters for the input uncertainty that satisfy all the constraints for the CIs of mean and standard deviation.

For the proposed RDO method, random sample sets that are generated using the uncertainty characterization results. The variance of the response is evaluated using the combination of these random sample sets during the RDO. The proposed RDO method provides a robust optimal design of an electric machine considering the uncertainties caused by multiple components. The proposed methods were applied to a surface-mounted permanent magnet synchronous motor (SPMSM) to be used in an EPS system to identify the uncertainty and reduce the cogging torque.

The remainder of the paper is organized as follows. In the next section, the cogging torque that is generated in the SPMSM is described. Section III explains the kriging surrogate modeling method. Section IV elucidates the uncertainty characterization using the bootstrap method and its results. Then, the proposed sample-based RDO method under uncertainties caused by multiple components is described and its results with regard to the SPMSM are discussed in Section V, and the conclusion is presented in Section VI.

II. Cogging Torque of SPMSM

A. Theoretical Background

The cogging torque is an undesirable torque caused by the interaction between the permanent magnets of the rotor and the stator slots in a permanent magnet electric machine. Owing to the stator slotting, the air gap varies periodically. This leads to a change in permeance at the air gap and a periodic oscillation in the magnetic energy. Thus, a pulsating torque is generated, even under no-load operation. This phenomenon is especially prominent at a low speed. The cogging torque is a periodic function that is a sum of the interactions between each edge of the rotor and stator slot openings. The harmonic components of the cogging torque can be classified based on their origins into native harmonic components (NHCs) and additional harmonic components (AHCs). NHCs always exist and inevitably occur even in an ideal electric machine. The NHCs can be easily obtained from an FEA. AHCs are usually generated in mass-produced electric machines owing to uncertainties caused by the manufacturing process. As the AHCs of the cogging torque are unpredictable at the initial design stage and considered negligible, reducing the NHCs of the cogging torque has been the main objective in electric machine design [8].

TABLE I
Specifications of SPMSM

Name	Unit	Value
No. of poles	-	6
No. of slots	-	9
Diameter of stator	mm	85
Skew	-	Three-step skew

A popular method for reducing cogging torque is to skew stator stacks or magnets. The main harmonic order (n_{mh}) of the cogging torque is calculated using the least common multiple (LCM) of the magnetic poles and the number of teeth on the stator, as given below:

$$n_{mh} = \mathrm{LCM}\left(Q, P\right), \tag{1}$$

where Q is the number of slots in the stator, and P is the number of poles in the rotor. The orders of the NHCs (N_{NHCi}) of the cogging torque are multiples of the main harmonic order.

$$N_{NHCi} = n_{mh} \cdot i, (i = 1, 2, 3, \cdots). \tag{2}$$

The elimination of the first few multiples of the main harmonic order is important because the magnitude of the cogging torque considerably decreases as the order increases. The skew angle applied to the rotor core can eliminate these harmonic components. The orders of the remaining NHCs (N_{NHCRi}) are

$$N_{NHCRi} = n_{mh} \cdot N_S \cdot i, (i = 1, 2, 3, \cdots), \tag{3}$$

where N_S is the number of steps.

The specifications of the SPMSM for the EPS system used in this study are listed in Table I. The SPMSM had six poles and nine slots and included a three-step skew rotor. The cogging torque was generated 18 times per rotation. The 18th- and 36th-order harmonic components were eliminated owing to the three-step skew, whereas the 54th-order harmonic component remained. The harmonic components that had an order higher than 54 were neglected because of their small magnitudes. The magnitude of the cogging torque reduced from 24.2 to 0.5 mNm owing to the three-step skew [8].

B. Experiment Using Prototypes

A total of six prototypes were fabricated to verify the cogging torque for the current design of the SPMSM. As a divided core was adopted, the size of the SPMSM was reduced owing to a high fill factor and short end-turn length. The productivity was also improved because of the easier winding. The fabricated prototypes and the measuring equipment for the cogging torque are shown in Fig. 1. The cogging torque of the prototypes was measured using a torque sensor. The measured results were validated through a second experiment using an additional sensor. The difference between the two measured cogging torques was less than 5%. Thus, the measured cogging torque of the prototypes was considered reliable. The results of the harmonic analysis of the measured cogging torque are shown in Fig. 2. Although the 6th- and 9th-order harmonic components of the cogging torque were expected to not appear, these components

Fig. 1. Fabricated prototypes of SPMSM and measuring equipment [8].

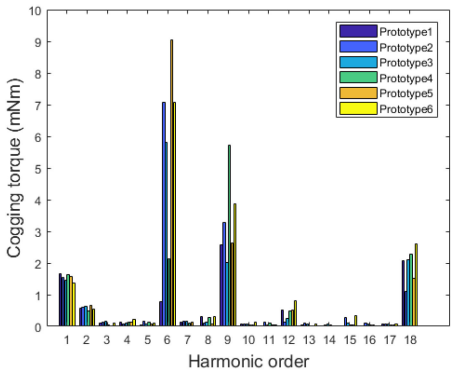

Fig. 2. Results of harmonic analysis of the measured cogging torque [14].

were significantly large. Therefore, AHCs cannot be neglected in manufactured electric machines. To examine the effects of various uncertainties on the generation of AHCs, a parametric study was previously performed for this SPMSM model [8]. However, only the effects of certain levels of uncertainties were investigated in the previous study, and these uncertainties were not characterized.

C. Effects of Uncertainties From Multiple Components

Most studies regarding the analysis and design optimization of electric machines and drives use a symmetry model for FEA to reduce computational time. In addition, conventional RDO methods involve one random variable for each uncertainty source. Accordingly, the combined effect of uncertainties from multiple components cannot be considered in conventional RDO methods. However, the cogging torque in the SPMSM can drastically change as uncertainties are considered as different random variables using a full model in the FEA. The 6th-order and 9th-order AHCs significantly affected the increase in the cogging torque [14]. However, the experimental results showed that the 6th-order AHC has a larger mean and variance. Therefore, the reduction in the 6th-order AHC was investigated in this study. The stator gap, which occurs on the surface of segmented stators, is a dominant factor that significantly affected the generation of the 6th-order AHC of the cogging torque [14]. To examine the combined effect of uncertainties caused by multiple stator gaps, two case studies were performed. First, the stator gaps were treated as a single random variable, and a full model was used for a fair comparison. A total of 9 levels from 0.01 mm to 0.09 mm were considered. Second, all the stator gaps were considered as different random variables. The stator gap was assumed to follow a normal distribution with a mean of 0.05 mm and a standard deviation of 0.005 mm, and the values were randomly generated.

Table II lists the results of the case study for the 6th-order AHC of the cogging torque. The magnitude of the 6th-order AHC was nearly negligible when the uncertainty was treated as a single random variable while it was significantly large when the uncertainties were treated as different random variables. The results indicate that even though there is a single source of uncertainty, the uncertainties from multiple components should be considered as different random variables to accurately predict the cogging torque; furthermore, the FEA using a full model is essential.

III. Surrogate Model

Before we characterize the input uncertainty and apply RDO to the SPMSM for the EPS, it is necessary to briefly understand surrogate modeling. A surrogate model is a functional relationship between the input design variable or parameter domain and the response [15]. The surrogate model is widely adopted in the design optimization of electric machines and drives to reduce the high computational cost associated with simulation [1], [2]. The surrogate modeling procedure comprises three steps: design of experiment (DOE), surrogate modeling, and validation of the surrogate model. There are several options, with regard to each step, that can be selected according to the characteristics of the problem, comfortability, accuracy, and computational cost. The details regarding the theories of surrogate models or their comparative study are beyond the scope of this paper. Therefore, a brief explanation of the selected methods will be given along with some prevalent references.

A. Design of Experiment

The DOE is the sampling plan in the input design variable or parameter domain. The DOE for surrogate modeling based on the response from deterministic computer simulation is different from the one based on the response from real-world experimentation [16], [17]. DOE techniques are required to satisfy the following properties: granularity, space-filling, non-collapsing property, and orthogonality [18].

In this study, a combination of optimal Latin hypercube design (OLHD) and sequential maximin distance design (SMDD) was implemented [14], [19]. The main objective of OLHD was to obtain design points that satisfy the space-filling and non-collapsing properties in the design domain [20]. Then, SMDD was applied based on the design points obtained from the OLHD by sequentially adding one design point at a time. The maximin distance criterion was used in the SMDD to guarantee sufficient design points at the boundaries and empty space in the design domain [21]. Both DOE techniques were applied to the normalized design domain in the range of [0,1].

TABLE II
RESULTS OF THE CASE STUDY

	Stator gap	1	2	3	4	5	6	7	8	9
Full model	1, …, 9	0.0100	0.0200	0.0300	0.0400	0.0500	0.0600	0.0700	0.0800	0.0900
6th-order harmonic component (×10^{-3} mNm)		0.5396	1.4526	3.2882	6.4262	10.7304	16.0392	7.8544	11.2699	18.3766
Full model	1	0.0549	0.0492	0.0679	0.0587	0.0567	0.0424	0.0545	0.0286	0.0525
	2	0.0662	0.0637	0.0258	0.0171	0.0515	0.0309	0.0560	0.0497	0.0612
	3	0.0651	0.0589	0.0496	0.0152	0.0624	0.0443	0.0361	0.0416	0.0459
	4	0.0402	0.0553	0.0208	0.0512	0.0580	0.0597	0.0473	0.0827	0.0736
	5	0.0539	0.0688	0.0653	0.0358	0.0635	0.0624	0.0180	0.0671	0.0428
	6	0.0358	0.0639	0.0629	0.0562	0.0480	0.0348	0.0672	0.0125	0.0549
	7	0.0302	0.0536	0.0500	0.0602	0.0478	0.0429	0.0406	0.0566	0.0600
	8	0.0639	0.0396	0.0489	0.0629	0.0651	0.0521	0.0319	0.0290	0.0513
	9	0.0500	0.0402	0.0127	0.0396	0.0181	0.0456	0.0462	0.0462	0.0632
6th-order harmonic component (mNm)		9.0945	11.0532	11.5793	12.9681	24.4431	9.6392	7.2857	6.4532	7.6828

B. Kriging Surrogate Model

Several surrogate models, such as response surface model, support vector machine, radial basis function, artificial neural network, and kriging surrogate model, have been applied to the design optimization of electric machines and drives [1], [2]. Although each model has its advantages and disadvantages, all the models have been successfully implemented for the design optimization of electric machines and drives. In this study, the kriging surrogate model was selected because of its high accuracy with regard to both linear and nonlinear responses and owing to its ability to perform reliable predictions [22], [23]. The kriging surrogate model is defined as the sum of a global model and a local model [24], [25].

$$\hat{Y}(\boldsymbol{x}) = \boldsymbol{f}(\boldsymbol{x})^T \hat{\boldsymbol{\beta}} + \boldsymbol{r}(\boldsymbol{x})^T \boldsymbol{R}^{-1} \left(\boldsymbol{Y} - \boldsymbol{F}\hat{\boldsymbol{\beta}} \right), \tag{4}$$

where $\boldsymbol{f}(\boldsymbol{x})$ is the vector of known regression functions, $\hat{\boldsymbol{\beta}}$ is the vector of estimators of unknown regression coefficients, $\boldsymbol{r}(\boldsymbol{x})$ is the correlation vector between the design points and prediction point, $\boldsymbol{R}$ is the correlation matrix between the design points, $\boldsymbol{Y}$ is the response vector at design points, and $\boldsymbol{F}$ is the expanded design matrix. The first component, which is the estimator of the global model, is determined using the generalized least squares method. The second component, which is the local model, is the deviation from the estimated mean model. The correlation matrix, which is included in the local model, is defined by a correlation function. Among various correlation functions, the Gaussian correlation function is widely adopted because it smoothly interpolates the response.

$$\boldsymbol{R}\left(\boldsymbol{\theta}, \boldsymbol{x^i}, \boldsymbol{x^j}\right) = \exp\left(\sum_{k=1}^{n_d} -\theta_k \left(x_k^i - x_k^j \right)^2 \right), \tag{5}$$

where $\boldsymbol{x^i}$ and $\boldsymbol{x^j}$ are the vectors of design points *i* and *j*, respectively, $\boldsymbol{\theta}$ is the correlation coefficient vector, and n_d is the dimension of the domain. The correlation coefficients are estimated using maximum likelihood estimation.

C. Validation of Surrogate Model

Assessing the quality of the surrogate model is an important step in employing surrogate modeling in design optimization. To validate a surrogate model, an error measure and validation method should be determined. The error measure represents the accuracy of a surrogate model, and the validation method deals with the evaluation of the error measure using the given design points and the response values. The normalized root mean square error (NRMSE) and leave-one-out cross-validation method were used in this study [14], [15]. The leave-one-out cross-validation method leaves out one design point for validation and uses the others to construct the surrogate model. The NRMSE based on the leave-one-out cross-validation method is defined as

$$\text{NRMSE} = \sqrt{\frac{1}{n_s} \sum_{i=1}^{n_s} \left(\frac{\hat{Y}_{-i}(x_i) - Y(x_i)}{\max(\mathbf{Y}(\mathbf{x})) - \min(\mathbf{Y}(\mathbf{x}))} \right)^2} \times 100, \tag{6}$$

where n_s is the number of design points, $\hat{Y}_{-i}(x_i)$ is the predicted response at the *i*th design point obtained from the kriging surrogate model that is constructed by leaving out the *i*th design point from training, $Y(x_i)$ is the response at the *i*th design point calculated from the simulation model, and $\max(\mathbf{Y}(\mathbf{x}))$ and $\min(\mathbf{Y}(\mathbf{x}))$ are the maximum and minimum response values, respectively, among those at the design points.

IV. UNCERTAINTY CHARACTERIZATION

The knowledge of the probability distribution and its statistical parameters of input uncertainties is an important prerequisite for applying probabilistic design optimization techniques. In many engineering applications, the direct measurement of input parameters, i.e. manufacturing and assembly tolerance, and material properties of the prototypes may be extremely challenging

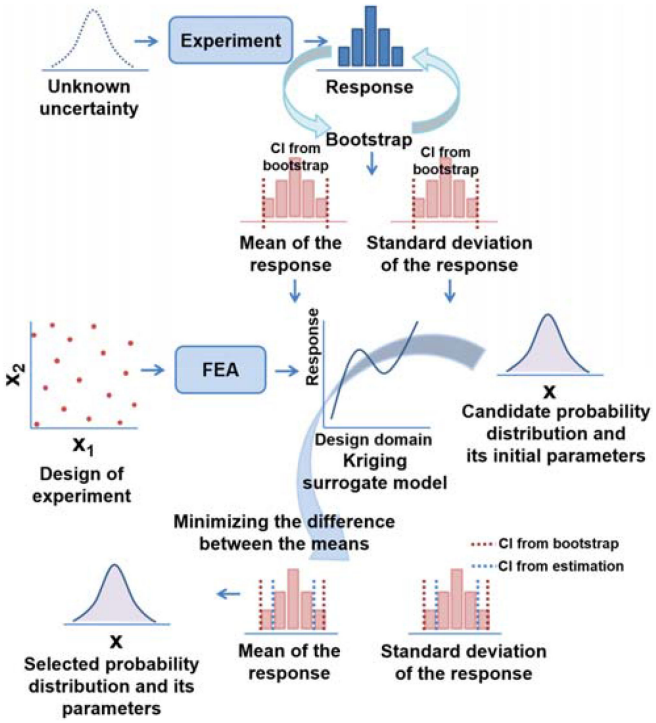

Fig. 3. Procedure of uncertainty characterization using the bootstrap method.

and expensive. The measurement of responses is an easier approach and may be the only feasible option. The inverse problem is generally solved by identifying the probability distribution and estimating its statistical parameters of input uncertainties from the response measurements. This is known as uncertainty characterization or identification. However, conventional methods such as perturbation method and Monte Carlo simulation (MCS) are less accurate because of the linearization of the response or the requirement of numerous computations [26], [27].

This study proposes an uncertainty characterization method that is computationally efficient, while maintaining accuracy. To consider the lack of information owing to the limited number of prototypes, the bootstrap method was implemented to predict the CIs of sample estimates. The procedure of the proposed uncertainty characterization using the bootstrap method is described in Fig. 3. First, the response data were collected via the measuring experiment of the prototypes. The CIs of the mean and standard deviation were obtained using the bootstrap method. Second, the kriging surrogate model was constructed based on the response obtained from the FEA. The design points were determined based on a DOE technique. Subsequently, to minimize the difference between the mean values obtained from the prototypes and response data, the unknown probability distributions and the statistical parameters of input uncertainty were assumed based on the candidate distribution list and initial design. A total of 200 random samples were generated, and the response data were calculated using the kriging surrogate model. Using these response data, the CIs of the mean and standard deviation were obtained. The minimization between the mean values from the prototypes and the response data was performed. The CIs of the mean and standard deviation obtained from the uncertainty characterization were set to be within those obtained from the bootstrap method using experimental data. The probability distribution of the input uncertainty that minimizes the objective function while satisfying the constraints was selected. Therefore, the mean and standard deviation of the response were estimated through optimization using the kriging surrogate model. As the 6th-order AHC significantly contributes to the increased cogging torque, the uncertainty of the stator gap was characterized in this study. Although there is only one source of uncertainty, the number of input uncertainties is nine, as the SPMSM has nine slots. Therefore, the probability distribution and its statistical parameters for the uncertainty of the stator gap should be characterized using nine input parameters.

A. CI from the Bootstrap Method

A large number of prototypes leads to increased accuracy and precision when estimating the statistical parameters of a probability distribution. The number of prototypes is generally determined based on the available time and budget. Considering that only one prototype is usually fabricated for experiment or design verification, the experimental results of six prototypes can provide more useful information. As the number of prototypes was still small, we needed to consider all the possibilities that can occur in the production based on these prototypes. To account for this lack of information, the bootstrap was adopted [28]. The bootstrap has been used in many fields of science and engineering to evaluate the CI for an estimator, for instance, mean and standard deviation, when only few data are available [29], [30]. Among various bootstrap methodologies, the bootstrap quantile interval was adopted in this study. This method is based on the percentiles of the distribution of the bootstrap replicates. The advantage of this method is that it can conservatively predict the variation in the cogging torque based on the CI for the estimators. The steps involved in calculating the bootstrap percentile interval are [31]:

1) Given a random sample, $\mathbf{x} = (x_1, \cdots, x_n)$, calculate $\hat{\theta}$.
2) Sample with replacement from the original sample to obtain $\mathbf{x}^{*b} = (x_1^{*b}, \cdots, x_n^{*b})$
3) Calculate the same statistic using the sample in the step 2 to obtain the bootstrap replicates, $\hat{\theta}^{*b}$.
4) Repeat steps 2 through 3 B times, where $B \geq 1000$.
5) Order the $\hat{\theta}^{*b}$ from the smallest to the largest.
6) Calculate $B \cdot \alpha/2$ and $B \cdot (1 - \alpha/2)$.
7) The lower endpoint of the interval is given by the bootstrap replicate that is in the $B \cdot \alpha/2^{\text{th}}$ position of the ordered $\hat{\theta}^{*b}$, and the upper endpoint is given by the bootstrap replicate that is in the $B \cdot (1 - \alpha/2)^{\text{th}}$ position of the same ordered list.

The bootstrap percentile CI is as follows:

$$\left(\hat{\theta}_B^{*(\alpha/2)}, \hat{\theta}_B^{*(1-\alpha/2)}\right), \tag{7}$$

where $\hat{\theta}_B^{*(\alpha/2)}$ and $\hat{\theta}_B^{*(1-\alpha/2)}$ are the $\alpha/2$ and $1 - \alpha/2$ quantiles in the bootstrap distribution of $\hat{\theta}^*$, respectively. For example, if $\alpha = 0.05$ and $B = 1000$, then $\hat{\theta}_{1000}^{*(0.025)}$ is the $\hat{\theta}^{*b}$ in the 25th

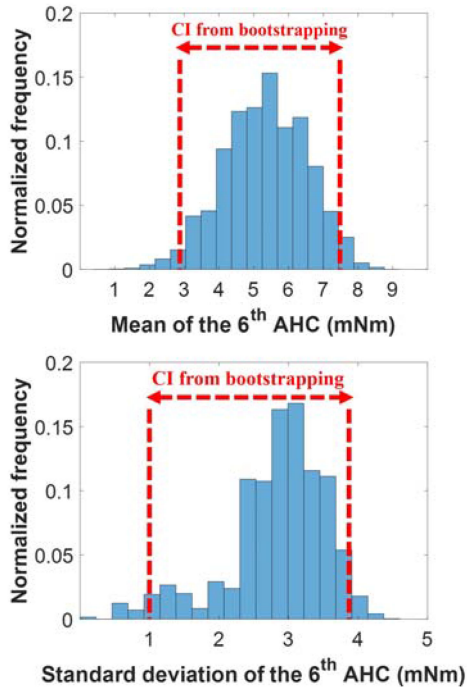

Fig. 4. CIs of mean and standard deviation from the bootstrap method based on experimental data.

TABLE III
CONFIDENCE INTERVAL OF MEAN AND STANDARD DEVIATION OBTAINED FROM THE BOOTSTRAP METHOD

Estimator	Lower endpoint	Upper endpoint
Mean ($\hat{\mu}^*$)	$\hat{\mu}_L^* = 2.8896$	$\hat{\mu}_U^* = 7.5212$
Standard deviation ($\hat{\sigma}^*$)	$\hat{\sigma}_L^* = 1.0211$	$\hat{\sigma}_U^* = 3.9100$

position in the ordered list of bootstrap replicates. Similarly, $\hat{\theta}_{1000}^{*(0.975)}$ is the replicate in the 975th position. In this study, the level of significance (α) is 0.05, and the number of resampling (B) is 10^5. The histograms in Fig. 4 show the bootstrap replicates of the mean and standard deviation. The dotted lines denote the lower and upper endpoints of the CIs of mean and standard deviation that were obtained from the bootstrap method. The histograms were normalized using the total number of resampled data obtained from bootstrapping. Table III lists the corresponding lower and upper endpoints of CIs of mean and standard deviation.

B. Kriging Surrogate Model

To reduce the computational cost of the repetitive FEA simulation during optimization in uncertainty characterization, the kriging surrogate model was adopted. The combination of the OLHD and SMDD was used in the DOE. The number of design points for the OLHD and SMDD was 275 respectively, which is five times larger than the saturated number for the 9th-dimensional domain [19]. The NRMSE, which was used as the error measure, and the leave-one-out cross-validation method was employed to validate the kriging surrogate model.

TABLE IV
UNCERTAINTY CHARACTERIZATION RESULTS

Identified probability distribution	Location parameter	Scale parameter
Weibull distribution	$\lambda = 0.0698$	$k = 13.8702$
Estimator	Estimated value	Bootstrap
Mean	$\hat{\mu} = 7.2593$	$\hat{\mu}^* = 5.3211$
CI	Lower endpoint	Upper endpoint
$\hat{\mu}$	$\hat{\mu}_L = 7.1014$	$\hat{\mu}_U = 7.4141$
$\hat{\sigma}$	$\hat{\sigma}_L = 1.0211$	$\hat{\sigma}_U = 1.2434$

The NRMSE of the kriging surrogate model was 6.11%. The level of error was acceptable considering that the number of design points was small and the dimensionality of the problem was high.

C. Proposed Method and Results

The proposed uncertainty characterization method identifies the probability distribution and estimates its statistical parameters based on the bootstrap method, which is applied to the experimental data and kriging surrogate model constructed using the FEA simulation. The candidate probability distributions for the unknown input uncertainty are as follows: normal, log-normal, gamma, Weibull, and maximum Gumbel distributions. The uncertainty characterization was performed by solving the following optimization problem:

$$\begin{aligned} &\min_{a,b} |\hat{\mu} - \hat{\mu}^*| \\ &\text{s.t. } \hat{\mu}_L^* \le \hat{\mu}_L \cdot \\ &\quad \hat{\mu}_U \le \hat{\mu}_U^* \cdot \\ &\quad \hat{\sigma}_L^* \le \hat{\sigma}_L \cdot \\ &\quad \hat{\sigma}_U \le \hat{\sigma}_U^*, \end{aligned} \tag{8}$$

where $\hat{\mu}$ and $\hat{\mu}^*$ are the mean values of the 6th-order AHC of the cogging torque obtained from the estimation and bootstrap replicates, a and b are the statistical parameters of the candidate probability distribution, $\hat{\mu}_L^*$ and $\hat{\mu}_U^*$ are the lower and upper endpoints of the mean obtained from the bootstrap method, $\hat{\sigma}_L^*$ and $\hat{\sigma}_U^*$ are the lower and upper endpoints of the standard deviation obtained from the bootstrap method, $\hat{\mu}_L$ and $\hat{\mu}_U$ are the lower and upper endpoints of the mean obtained from the estimation, and $\hat{\sigma}_L$ and $\hat{\sigma}_U$ are the lower and upper endpoint of the standard deviation obtained from the estimation. The sequential quadratic programming optimization algorithm in MATLAB was used in this study [32]. As the percentile bootstrap interval provides a highly conservative CI, the constraints ensure that the CI obtained from the simulation is located within these boundaries [28], [31].

The uncertainty characterization results are listed in Table IV. The probability distribution of the stator gap, obtained from the uncertainty characterization, is shown in Fig. 5 for the

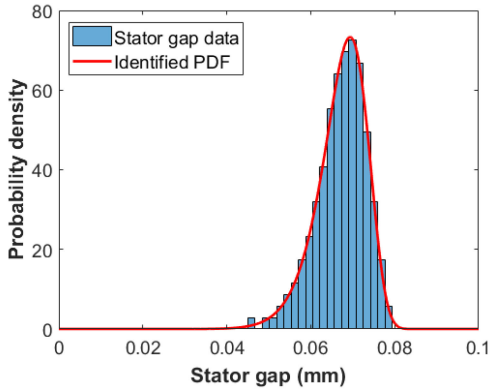

Fig. 5. Probability distribution of the stator gap for the 6th-order AHC of the cogging torque resulting from the uncertainty characterization.

6th-order AHC of the cogging torque. The difference between the mean values obtained from the bootstrap method based on the experimental data and the uncertainty characterization was 1.9367. The constraints were also satisfied as the estimated CIs of the mean and standard deviation were within those obtained from the bootstrap method. The CIs of the mean and standard deviation obtained from the uncertainty characterization were narrower than those obtained from the bootstrap method. This is a reasonable result because the CIs obtained from the experiment were obtained using only few prototypes, and they were conservatively evaluated. The CI of the standard deviation closely converged to the lower boundary. This means that some other neglected factors other than the stator gap may exist. This is beyond the scope of this study. Nevertheless, we believe that the proposed RDO considering only the uncertainty of the stator gap can yield a more robust design than the current design. The probability distribution for the stator gap was identified as Weibull distribution and its location and scale parameters were estimated as 0.0698 and 13.8702, respectively. The uncertainty characterization results show that there is a significant amount of stator gaps close to 0.0698 mm and its probability distribution is slightly right-skewed. The maximum Gumbel distribution was excluded because it had a long right tail that generates samples larger than 0.1mm.

V. Robust Design Optimization

In RDO, robustness is added to deterministic design optimization. One of the most popular and widely used conventional RDO methods formulates the sum of the mean and variance of the response as the objective function and evaluates the mean and variance using the Taylor series expansion [3].

$$\mu_f \cong f\left(\boldsymbol{\mu}_{\boldsymbol{x}^b}, \boldsymbol{\mu}_{\boldsymbol{x}^p}\right) \tag{9}$$

$$\sigma_f^2 \cong \sum_{i=1}^{n} \left(\frac{\partial f}{\partial x_i^b}\right)^2 \sigma_{x_i^b}^2 + \sum_{i=1}^{m} \left(\frac{\partial f}{\partial x_i^p}\right)^2 \sigma_{x_i^p}^2, \tag{10}$$

where $\boldsymbol{x}^b$ and $\boldsymbol{x}^p$ are design variables that are controlled by the designers and design parameters that are constant vectors, respectively, $\boldsymbol{\mu}_{\boldsymbol{x}^b}$ and $\boldsymbol{\mu}_{\boldsymbol{x}^p}$ are the mean vectors of the design variable and parameter, $\sigma_{x_i^b}^2$ and $\sigma_{x_i^p}^2$ are the variance of each design variable and parameter, f is the response function, and μ_f and σ_f^2 are the mean and variance of the response function. The conventional RDO methods applied to electromagnetic devices have used a symmetry model for FEA to calculate the response. With regard to the design of electric machines and drives, several uncertainties in design parameters can arise from a single source of uncertainty. This can lead a significant error if only one random variable is employed. In the RDO of the SPMSM, nine random variables, which are the uncertainties of the stator gap, should be implemented because of the multiple components. As the conventional RDO approximates the variance or standard deviation using the first-order Taylor series expansion, the first-order partial derivatives of the response function should be evaluated. This can drastically increase the computational cost as the FEA of the full model of the electric machines and drives should be repetitively performed.

To tackle this challenging issue, this study proposes a sample-based RDO method using the kriging surrogate model. First, a total of 200 random sample sets were generated based on the results of the proposed uncertainty characterization. Second, the kriging surrogate model was constructed based on the response values obtained from the FEA. The design points were determined based on the combination of the OLHD and SMDD. Next, the response sets were evaluated using the kriging model. Finally, the mean and standard deviation were calculated using these response sets. The combination of the random sample sets for the uncertainty of the stator gap is illustrated in Fig. 6. A substantial advantage of the proposed method is that the mean and standard deviation of the response are evaluated directly using the random sample sets without any approximations and there is no additional computational cost as the dimension of the problem increases.

The RDO of the SPMSM is formulated as follows:

$$\begin{aligned} &\min_{\mathbf{x}} \; F\left(\mu\left(T_{p-p}\right), \sigma\left(T_{p-p}\right)\right) \\ &\text{s.t. } BEMF \geq BEMF^t \\ &\quad T_{AHC6} \leq T_{AHC6}^t, \end{aligned} \tag{11}$$

where T_{p-p} is the peak-to-peak value of the cogging torque, F is the sum of the mean and standard deviation of the peak-to-peak value of the cogging torque, $BEMF$ is the back electromotive force and $BEMF^t$ is the target value of $BEMF$, T_{AHC6} is the 6th-order AHC of the cogging torque and T_{AHC6}^t is the target value of T_{AHC6}. $BEMF^t$ is set based on the requirement of the company and T_{AHC6}^t is the upper endpoint of the CI obtained from the uncertainty characterization. There are six design variables: yoke width (x_1), slot opening width (x_2), tooth tip (x_3), permanent magnet thickness (x_4), pole angle (x_5), and rotor eccentricity (x_6). The design parameter is the stator gap. There are nine random variables of the design parameters considered in this RDO problem arising from the uncertainty of the stator gap. The design variables and parameters are illustrated in Fig. 6. The uncertainties of design variables were not considered because they were not significant for the response of the SPMSM. The local sensitivity was evaluated with the

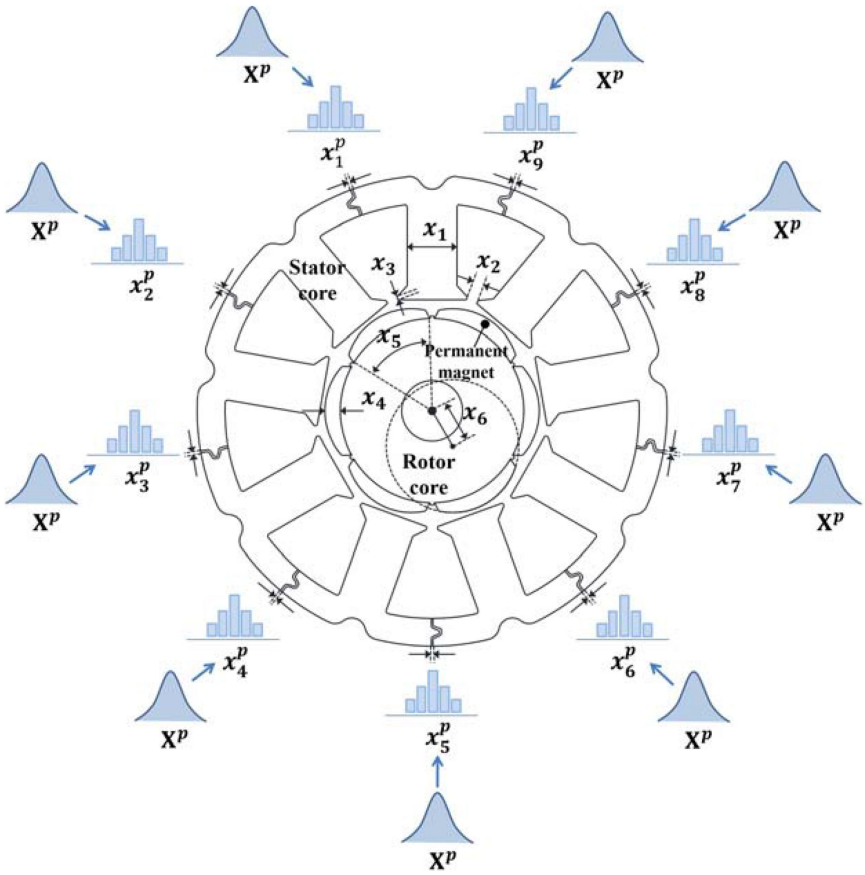

Fig. 6. Combination of random sample sets for the uncertainty of the stator gap used in the proposed sample-based RDO method for the SPMSM.

TABLE V
LOCAL SENSITIVITY ANALYSIS OF DESIGN VARIABLES/PARAMETERS

Design variable/parameter	Local sensitivity		
	T_{AHC6}	T_{p-p}	$BEMF$
x_1	0.0047	0.0344	0.0001
x_2	0.0388	1.1885	0.0044
x_3	0.0468	0.3444	0.0008
x_4	0.1072	2.7925	0.9748
x_5	0.2338	1.7220	0.0038
x_6	0.0228	1.3865	0.2424
x_7	215.0118	465.1413	0.6492

TABLE VI
INITIAL AND ROBUST OPTIMAL DESIGN OF THE SPMSM

Input/output		Initial design	Robust optimal design
Design variable	x_1	0.5	1
	x_2	0.5	0.2511
	x_3	0.5	0.0810
	x_4	0.5	0.0695
	x_5	0.5	1
	x_6	0.5	0.1511
Response	$\mu[T_{p-p}]$ (mNm)	19.8811	16.7622 (MCS: 16.7608)
	$\sigma[T_{p-p}]$ (mNm)	2.6412	1.1375 (MCS: 1.1885)
	$BEMF$ (V_{rms})	8.6997	8.0000 (MCS: 8.0000)
	T_{AHC6} (mNm)	9.6699	7.5212 (MCS: 7.5213)

absolute value of the partial derivative with respect to each design variable and parameter [33], and its results are listed in Table V. As the stator gap was the most significant design parameter, the uncertainties of the stator gap were considered in RDO and the uncertainties of other design variables were considered negligible.

To decrease the numerical cost of the repetitive FEA simulation during the RDO, the kriging surrogate model was employed. The same surrogate modeling procedure as the one used in the uncertainty characterization was employed. The combination of the OLHD and SMDD was used for the DOE. The number of design points used for each DOE method was 680. Thus, 1360 design points were used for surrogate modeling. Three kriging surrogate models were constructed for T_{p-p}, $BEMF$,

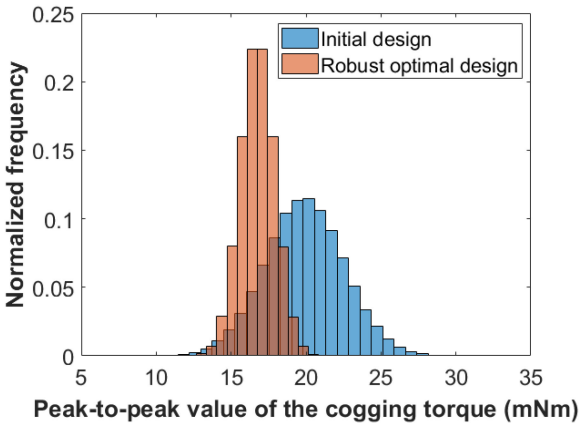

Fig. 7. Peak-to-peak value of the cogging torque of the initial and robust optimal design.

and T_{AHC6}. The NRMSE of each kriging surrogate model was 9.45%, 3.17%, and 9.80% respectively. The levels of errors were acceptable considering the low number of design points for the surrogate model and high dimensionality.

The initial and robust optimal designs of the SPMSM are listed in Table VI. The design variables are normalized using min–max normalization. The real values of design variables are not disclosed in this study because they are proprietary information belonging to the sponsoring company. The min–max normalization brings all the values of the design variables into the range of [0,1] using the lower and upper boundaries of each design variable. The initial design showed a large peak-to-peak value of the cogging torque with a certain level of standard deviation. The RDO found a robust optimal solution that significantly reduced the mean and standard deviation of T_{p-p} by 15.68% and 56.93%, respectively. T_{AHC6} significantly decreased by 22.22% compared to that of the initial design and converged to the target value. The $BEMF$ slightly decreased by 8.04% and became active. The peak-to-peak values of the cogging torque of the initial design and robust optimal design are shown in Fig. 7. As the validation of the RDO results through MCS using FEA requires extremely large computational time, the MCS using the kriging surrogate model was alternatively performed at the robust optimal design point. The number of random sample sets for MCS was 100,000. The errors of the means of T_{p-p}, $BEMF$, and T_{AHC6} were significantly small: 0.01%, 0%, and 0.01%, respectively. The error of the standard deviation of T_{p-p} was 4.29%. Although there is a significant difference between the standard deviation of the T_{p-p} and that in the case of the MCS, the RDO reduced both mean and standard deviation of T_{p-p}.

VI. Conclusion

Two new methodologies were developed to obtain the robust optimal design of the SPMSM: an uncertainty characterization using small number of prototypes and the bootstrap method, and a sample-based RDO using the kriging surrogate model. The present study is notable owing to two main contributions. First, the uncertainty is characterized using bootstrap percentile CIs, the kriging surrogate model and the optimization procedure based on few experimental data. Second, an RDO that uses random sample sets, which are generated from the identified probability distribution of the input uncertainty and enables efficient evaluation of the mean and standard deviation of responses is developed. The results of the application of the proposed method to the SPMSM show a significant improvement in its robustness and performance. As the uncertainty was characterized using experimental data obtained from several prototypes, the statistical information of the uncertainty was more reliable. The mean and standard deviation of the peak-to-peak value of the cogging torque were reduced by 15.68% and 56.93%, respectively, compared with those of the initial design. The RDO results were validated via the MCS, which showed that the errors were acceptably small.

References

[1] G. Lei, J. Zhu, and Y. Guo, *Multidisciplinary Design Methods for Electrical Machines and Drive Systems*. Berlin, Germany: Springer-Verlag, 2016.
[2] G. Lei *et al.*, "A review of design optimization methods for electrical machines," *Energies*, vol. 10, no. 12, Nov. 2017, Art. no. 1962.
[3] G. J. Park *et al.*, "Robust design: An overview," *AIAA J.*, vol. 44, no. 1, pp. 181–191, Jan. 2006.
[4] L. Gašparin *et al.*, "Additional cogging torque components in permanent-magnet motors due to manufacturing imperfections," *IEEE Trans. Magn.*, vol. 45, no. 3, pp. 1210–1213, Mar. 2009.
[5] I. Coenen *et al.*, "Manufacturing tolerances: estimation and prediction of cogging torque influenced by magnetization faults," *IEEE Trans. Magn.*, vol. 48, no. 5, pp. 1932–1936, May 2012.
[6] J. Jang *et al.*, "Reliability-based robust design optimization with kernel density estimation for electric power steering motor considering manufacturing uncertainties," *IEEE Trans. Magn.*, vol. 51, no. 51, Mar. 2015, Art. no. 8001904.
[7] J. Jang *et al.*, "Space-time kriging surrogate model to consider uncertainty of time interval of torque curve for electric power steering motor," *IEEE Trans. Magn.*, vol. 54, no. 3, Mar. 2018, Art. no. 8200804.
[8] J. Kim *et al.*, "Analysis of cogging torque caused by manufacturing tolerances of surface-mounted permanent magnet synchronous motor for electric power steering," *IET Power Electron.*, vol. 10, no. 8, pp. 691–696, Apr. 2016.
[9] G. Lei *et al.*, "Robust design optimization of PM-SMC motors for Six Sigma quality manufacturing," *IEEE Trans. Magn.*, vol. 49, no. 7, pp. 3953–3956, Jul. 2013.
[10] Z. Ren *et al.*, "New reliability-based robust design optimization algorithms for electromagnetic devices utilizing worst case scenario approximation," *IEEE Trans. Magn.*, vol. 49, no. 5, pp. 2137–2140, May 2013.
[11] Z. Ren *et al.*, "Numerically efficient algorithm for reliability-based robust optimal design of TEAM problem 22," *IEEE Trans. Magn.*, vol. 50, no. 2, Feb. 2014, Art. no. 7016304.
[12] B. Kang, K. K. Choi, and D. H. Kim, "An efficient serial-loop strategy for reliability-based robust optimization of electromagnetic design problems," *IEEE Trans. Magn.*, vol. 54, no. 3, Mar. 2018, Art. no. 7000904.
[13] H. G. Beyer and B. Sendhoff, "Robust optimization – A comprehensive survey," *Comput. Methods. Appl. Mech. Eng.*, vol. 196, no. 33–34, pp. 3190–3218, Jul. 2007.
[14] S. Kim *et al.*, "Uncertainty identification method using kriging surrogate model and Akaike criterion for industrial electromagnetic device," *IET Sci. Meas. Technol.*, vol. 14, no. 3, Apr. 2020.
[15] N. V. Queipo *et al.*, "Surrogate-based analysis and optimization," *Prog. Aerosp. Sci.*, vol. 41, no. 1, pp. 1–28, Jan. 2005.
[16] M. D. Mckay, R. J. Beckman, and W. J. Conover, "A comparison of three methods for selecting values of input variables in the analysis of output from a computer code," *Technometrics*, vol. 42, no. 1, pp. 55–61, Apr. 2000.
[17] J. P. C. Kleijnen *et al.*, "A user's guide to the brave new world of designing simulation experiments," *INFORMS J. Comput.*, vol. 17, no. 3, pp. 263–289, Aug. 2005.

[18] K. Crombecq, E. Laermans, and T. Dhaene, "Efficient space-filling and non-collapsing sequential design strategies for simulation-based modeling," *Eur. J. Oper. Res.*, vol. 214, no. 3, pp. 683–696, Nov. 2011.
[19] H. Kim *et al.*, "Efficient design optimization of complex system through an integrated interface using symbolic computation," *Adv. Eng. Softw.*, vol. 126, pp. 34–45, Dec. 2018.
[20] F. A. C. Viana, G. Venter, and V. Balabanov, "An algorithm for fast optimal Latin hypercube design of experiments," *Int. J. Numer. Meth. Eng.*, vol. 82, no. 2, pp. 135–156, Oct. 2010.
[21] M. E. Johnson, L. M. Moore, and D. Ylvisker, "Minimax and maximin distance designs," *J. Stat. Plan. Infer.*, vol. 26, no. 2, pp. 131–148, Oct. 1990.
[22] L. Lebensztajn *et al.*, "Kriging: A useful tool for electromagnetic device optimization," *IEEE Trans. Magn.*, vol. 40, no. 2, pp. 1196–1199, Mar. 2004.
[23] L. Wang and D. A. Lowther, "Selection of approximation models for electromagnetic device optimization," *IEEE Trans. Magn.*, vol. 42, no. 4, pp. 1227–1230, Apr. 2006.
[24] J. Sacks *et al.*, "Design and analysis of computer experiments," *Stat. Sci.*, vol. 4, no. 4, pp. 409–423, Nov. 1989.
[25] T. H. Lee and J. J. Jung, "Kriging metamodel based optimization," in *Optimization of Structural and Mechanical Systems*, Singapore, Singapore: World Scientific, 2007, pp. 445–484.
[26] J. R. Fonseca *et al.*, "Uncertainty identification by the maximum likelihood method," *J. Sound Vib.*, vol. 288, no. 3, pp. 587–599, Dec. 2005.
[27] H. H. Khodaparast, J. E. Mottershead, and M. I. Friswell, "Perturbation methods for the estimation of parameter variability in stochastic model updating," *Mech. Syst. Signal Pr.*, vol. 22, no. 8, pp. 1751–1773, Nov. 2008.
[28] B. Efron and R. Tibshirani, *An Introduction to the Bootstrap*. New York, NY, USA: Chapman Hall, 1993.
[29] A. M. Zoubir and B. Boashash, "The bootstrap and its application in signal processing," *IEEE Signal Proc. Mag.*, vol. 15, no. 1, pp. 56–76, Jan. 1998.
[30] V. Picheny, N. H. Kim, and R. T. Haftka, "Application of bootstrap method in conservative estimation of reliability with limited samples," *Struct. Multidiscip. Optim.*, vol. 41, no. 2, pp. 205–217, Mar. 2010.
[31] W. L. Martinez and A. R. Martinez, *Computational Statistics Handbook with MATLAB*. Boca Raton, FL, USA: Chapman Hall/CRC, 2002.
[32] J. S. Arora, *Introduction to Optimum Design*. Seoul, South Korea, Elsevier Korea L.L.C, 2017.
[33] G. Lei *et al.*, "Techniques for multilevel design optimization of permanent magnet motors," *IEEE Trans. Energy Convers.*, vol. 30, no. 4, pp. 1574–1584, Dec. 2015.

Saekyeol Kim received the bachelor's degree in mechanical engineering and a master's degree in automotive engineering from Hanyang University, Seoul, South Korea, in 2014 and 2016, respectively. Currently, he is pursuing a Ph.D. in automotive engineering from Hanyang University, Seoul, South Korea. His research interests include reliability design optimization, surrogate modeling, uncertainty quantification, statistical model calibration and validation, and design optimization of electric machines and drives.

Soo-Gyung Lee received the bachelor's degree in electrical engineering from Konkuk University, Seoul, South Korea, in 2014. Currently, she is pursuing a Ph.D. degree in automotive engineering from Hanyang University, Seoul. Her research interests include the design and optimization of electric machines.

Ji-Min Kim received the bachelor's degree in mechanical engineering and the Ph.D. degree in automotive engineering in 2009 and 2017, respectively, from Hanyang University, Seoul, Korea. Currently, he is working at Samsung electronics. His current research interests include the design and optimization of electric machine and analysis of noise and vibrations.

Tae Hee Lee (Member, IEEE) is a Professor at the Department of Automotive Engineering, Hanyang University, Seoul, South Korea. He serves as the General Council of IACM and Executive Committee of ASSMO. He received awards for Academic Excellence in Mechanical Engineering (2013) and in CAE and Applied Mechanics (2016) from KSME; in addition, he has received the Computational Mechanics Award from KSCM (2018). He was a Plenary Lecturer at CJK-OSM 8 (2014) and KSCM (2018) and a Semi-Plenary Lecturer at WCCM XII (2016) and APCOM (2019). His research interests include design optimization, design under uncertainty, surrogate model-based optimization, design and analysis of computer experiments, and data-driven design.

Myung-Seop Lim (Member, IEEE) received the bachelor's degree in mechanical engineering as well as the master's and the Ph.D. degree in automotive engineering from Hanyang University, Seoul, South Korea, in 2012, 2014, and 2017, respectively. From 2017 to 2018, he was a Research Engineer with Hyundai Mobis, Yongin, South Korea. In 2018, he was with Yeungnam University, Daegu, South Korea as an Assistant Professor. From 2019, he has been with Hanyang University, Seoul, South Korea, where he is currently an Assistant Professor. His research interests include electromagnetic field analysis and the design of electric machinery for mechatronics systems, such as automobiles and robotics.